

Surfaces and interfacial water: Evidence that hydrophilic surfaces have long-range impact

Jian-ming Zheng ^a, Wei-Chun Chin ^b, Eugene Khijniak ^c,
Eugene Khijniak Jr. ^a, Gerald H. Pollack ^{a,*}

^a Department of Bioengineering, Box 355061, University of Washington, Seattle, WA 98195, United States

^b School of Engineering, University of California, Merced, CA 95344, United States

^c Institute of Theoretical and Experimental Biophysics, Puschino, Russia

Available online 6 September 2006

Abstract

It is generally thought that the impact of surfaces on the contiguous aqueous phase extends to a distance of no more than a few water-molecule layers. Older studies, on the other hand, suggest a more extensive impact. We report here that colloidal and molecular solutes suspended in aqueous solution are profoundly and extensively excluded from the vicinity of various hydrophilic surfaces. The width of the solute-free zone is typically several hundred microns. Such large exclusion zones were observed in the vicinity of many types of surface including artificial and natural hydrogels, biological tissues, hydrophilic polymers, monolayers, and ion-exchange beads, as well as with a variety of solutes. Using microscopic observations, as well as measurements of electrical potential and UV–Vis absorption-spectra, infrared imaging, and NMR imaging, we find that the solute-free zone is a physically distinct and less mobile phase of water that can co-exist indefinitely with the contiguous solute-containing phase. The extensiveness of this modified zone is impressive, and carries broad implication for surface–molecule interactions in many realms, including cellular recognition, biomaterial–surface antifouling, bioseparation technologies, and other areas of biology, physics and chemistry.

© 2006 Published by Elsevier B.V.

Keywords: Water; Gel; Colloid; Hydrophilic surface; Interface

Contents

1. Introduction	20
2. Experimental observations and discussion	20
2.1. Generality	20
2.2. Unique physical characteristics of the exclusion zone.	23
2.3. Experimental procedures	25
2.3.1. Exclusion-zone observations	25
2.3.2. Exclusion of protein and fluorescein	25
2.3.3. Potential measurement	25
2.3.4. Spectrophotometer	25
2.3.5. MRI	26
2.3.6. Infrared radiation imaging	26
3. Conclusions.	26
Acknowledgments	26
References	26

* Corresponding author.

E-mail address: ghp@u.washington.edu (G.H. Pollack).

1. Introduction

Understanding the character of the near-surface aqueous zone is fundamental to an understanding how solutes interact with surfaces. Within such aqueous zones, solutes can sense surface features. Sensing interactions are generally thought to fall off within nanometers of the surface [1], although in colloidal systems studied in confined spaces, size-dependent depletion effects may extend by up to several particle diameters (e.g., [2,3]). Beyond this limited zone, surfaces are thought to be effectively invisible to solutes.

The older literature, on the other hand, reports much longer-range impact of surfaces. A 1949 review by Henniker [4] points to numerous experimental reports showing impressive long-range surface-induced ordering of various liquids, including water. More than 100 papers are cited. A book by Nobel Laureate Albert Szent-Gyorgyi [5] builds on this concept, presuming that long-range ordering of water is the essential foundation of bioenergetics, and a similar foundational concept forms the centerpiece of several major works on cell function (e.g., Ling, 1984 [6], Pollack, 2001 [7]).

While much of this older evidence has been forgotten, the modern literature is by no means devoid of reports of long-range effects. One of them is the presence of thermal anomalies in water, which penetrate substantial distances into aqueous solution (for review, *c.f.* Clegg and Drost-Hansen [8]). Another is the presence of solute-free “voids” in colloidal solute suspensions, with characteristic dimensions of 100 μm [9,10]. A third is based on interferometric measurements of polished quartz surfaces by Pashley and Kitchener [11] and Fisher et al. [12], which provide evidence that hydration could easily extend to several hundred water-molecule layers.

Two very recent papers once again raise the issue of long-range effects. On theoretical grounds Ling (2003) argues that under certain ideal conditions water ordering could extend virtually infinitely [13], while Roy et al. (2005) argue for long-range ordering based on precedent in the materials-science field [14]: In the case of semiconductor materials for example, surface substrates commonly order molten silicon into crystalline arrays; the ordering extends many molecular layers into the bulk without any transfer of substrate molecules. The same applies to the ordering of aluminum by aluminum-oxide surfaces. The commonality of such epitaxial ordering leads the authors to suggest the inevitability of similarly extensive surface-induced ordering of water molecules [14].

One obstacle to any thinking along the lines of possible long-range water ordering is how water molecules could be restricted to attain such order. Water molecules may readily adsorb onto hydrophilic surfaces through hydrogen bonding, but it is generally thought that additional ordering conferred by subsequent hydration layers that build onto the first will quickly give way due to the disruptive effects of thermal motion. Thus, while ample experimental precedent for long-range ordering is established, the reason why any such ordering could extend for long distances is not established.

To realize any such long-range stability, either hydrogen-bond energy holding molecules together would need to be higher

than expected, or thermal motion tending to rip them apart would need to be weaker than expected. The latter possibility is given force by observations on colloidal microspheres in aqueous suspension: At volume ratio of $\sim 1\%$, microsphere suspensions show two coexisting phases, random and crystalloid. In the random phase, thermal motion is of the anticipated magnitude, but in the crystalloid phase, although microspheres are distinctly separated from one another by several micrometers, r.m.s displacements are lower by an order of magnitude [15–17]. Thus, the disruptive effects of thermal motion in ordered regions may be less than generally anticipated, and this feature might predispose molecules to long-range ordering. In other words, any observations of long-range ordering might not necessarily violate foundational principles.

One way of examining the interfacial region is to explore the local disposition of solutes. If such interfacial water is genuinely in the ordered, liquid crystalline state, it is expected to exclude many solutes [6,18,19]. Recently, we confirmed that colloidal solutes are excluded from the near-surface zone of various gels, by distances on the order of 100 μm [20]. Although an extensive series of controls could rule out a variety of potential artifacts or trivial explanations [20], neither the basis, nor the generality of the observed exclusion phenomenon was evident from that study. Hence, we carried out the studies reported here, which demonstrate a role of hydrophilic surfaces more profound than presently considered.

2. Experimental observations and discussion

2.1. Generality

Examples of exclusion adjacent to a variety of surfaces are illustrated in the gallery of Fig. 1. Fig. 1a shows the disposition of microspheres in aqueous suspension some minutes after exposure to a polyacrylic-acid gel surface. Initially, the microspheres were dispersed throughout the aqueous phase. Progressively, they translated away from the gel surface, creating a particle-free zone that continued to expand at $\sim 1 \mu\text{m/s}$, leaving a stable $\sim 250 \mu\text{m}$ -wide particle-free zone. Whereas the polyacrylic-acid gel has a charged surface, similar results could be obtained with polyvinyl alcohol gels, which are not charged, implying that surface charge *per se* is not critical for exclusion.

Exclusion is not restricted to artificial gels alone, but also appears in the presence of biological tissues. Fig. 1b shows microsphere behavior in the vicinity of a representative biological specimen — muscle. Unlike the particle-free exclusion zones observed in the vicinity of artificial gels, the exclusion zone here was not absolute; it contained some microspheres, albeit in far lower concentration than in zones more remote. Exclusion zones have also been seen adjacent to collagen gels and vascular endothelium, using both microspheres and erythrocytes (data not shown).

To determine whether substrates with high water content (gels, biological tissues) are critical for the formation of exclusion zones, we examined thin polymeric specimens, where water efflux could play only a limited role. Fig. 1c shows an image of an optical fiber inserted into a suspension of microspheres. The

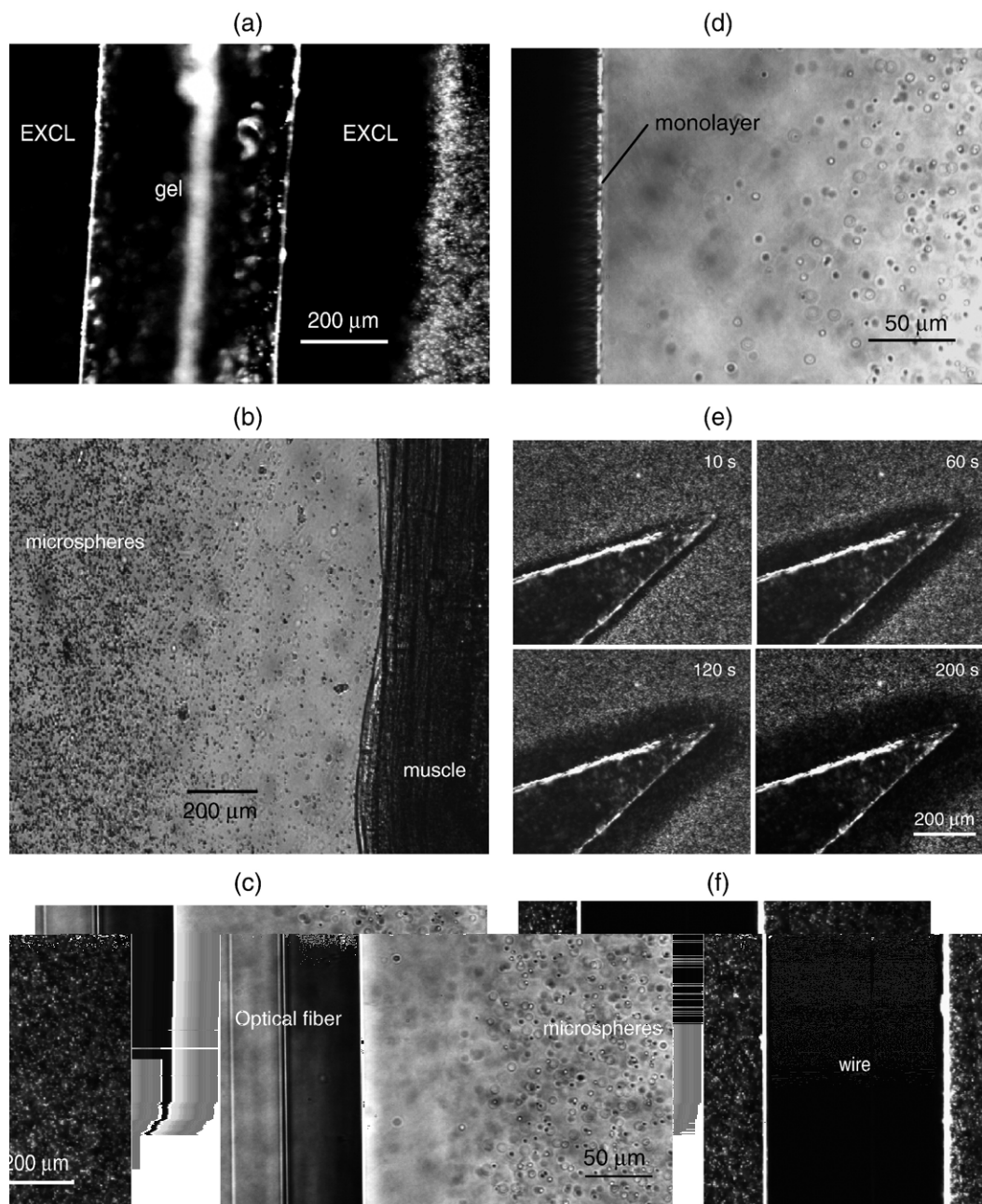


Fig. 1. Examples of solute exclusion from various interfaces. (a) Solute exclusion (EXCL) in the vicinity of polyacrylic acid gel. The gel was placed on a coverslip, superfused with a suspension of 1-μm carboxylate-coated microspheres, and observed in an inverted microscope (Zeiss Axiovert I35) equipped with a 20x objective. Image obtained 20 min. after superfusion. Microspheres (seen on right edge) undergo active thermal motion. (b) Microsphere exclusion in the vicinity of biological tissue. In eight specimens examined under similar conditions, the size of the exclusion zone, measured on video images, was found to be 360 ± 50 μm. (c) Optical fiber FS-SC-7324, Thorlabs, Newton, NJ (left) inserted into a microsphere suspension. Microspheres translate toward right. 20x objective, 2 μm carboxylate microspheres. (d) Hydrophilic monolayer, containing COOH groups. (e) Nafion-117 film, spear shaped, 170-μm thick, was sandwiched between two glass cover slips, much larger than the film. A carboxylated microsphere suspension 2-μm diameter was infiltrated around the sandwiched film. Dark zones are microsphere-free. Numbers in upper right indicate time after infiltration, in seconds. Only the first several minutes are shown. (f) Stainless steel wire sandwiched between two glass slides and exposed to microsphere suspension.

fiber contains an acrylate polymer coating. An exclusion zone of ~ 100 μm is seen with 1-μm carboxylate-functionalized microspheres, which carry negative charge groups. A similar exclusion zone was found with amidine-functionalized microspheres, which carry positive charge groups. Hence, the polarity of the solute is not a critical factor. Following acetone-mediated

dissolution of the polymer coating, the residual glass-fiber bundle showed no exclusion.

Exclusion was found also in the vicinity of a hydrophilic monolayer (Fig. 1d). The COOH-terminus monolayer covered a half-cylindrical zone on the outside of a glass capillary tube. The side without the monolayer showed no exclusion, while the side

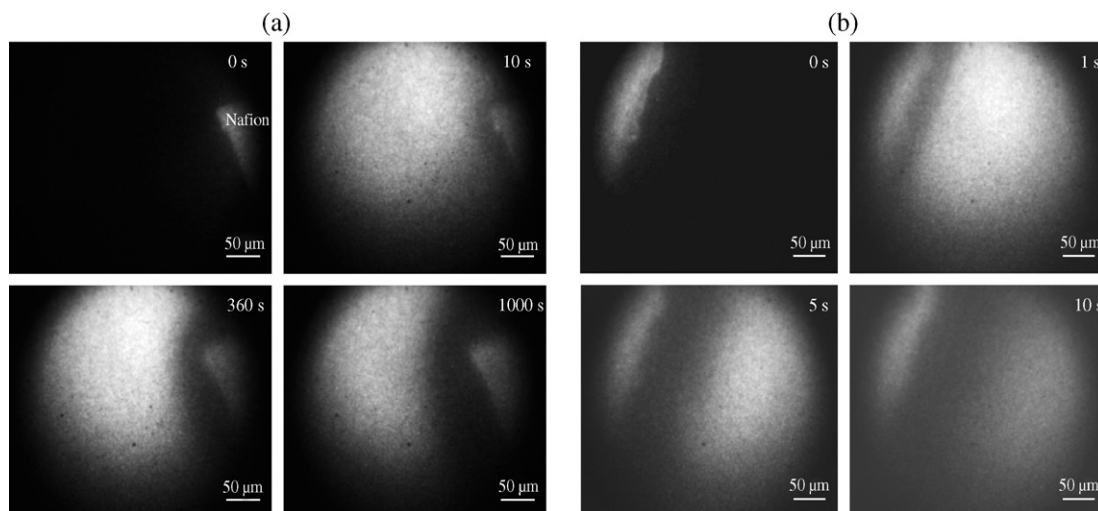


Fig. 2. a. Time course of exclusion of albumin, near a Nafion (upper right) surface. Note Nafion self-fluorescence. Protein added prior to second panel. b. Time course of exclusion of fluorescein dye from vicinity of Nafion (upper left). Dye added prior to second panel. Results show progressively widening stripe devoid of fluorescence (EXCL), reaching $\sim 100 \mu\text{m}$ within $\sim 10 \text{ s}$.

with the monolayer showed distinct exclusion, as shown. Similar results were obtained with several capillary tubes placed on the same slide, ruling out convection as a relevant factor. Full exclusion required several hours to develop, and the outer boundary of the exclusion zone was less distinct than with artificial gels (Fig. 1a).

Another polymer tested was the ionomer Nafion. Nafion is used broadly: as a proton-exchange membrane in electrodialysis, as a proton conductor in fuel cells, as a separator in electrolytic cells, and as a mechanical actuator [21]. It was considered especially interesting to study because interaction with water underlies many of its functions. Nafion-117 is composed of a carbon–fluorine backbone with perfluoro side chains containing sulfonic acid groups, fabricated from a copolymer of tetrafluoroethylene and perfluorinated monomers. The sulfonic acid groups confer hydrophilicity on an otherwise hydrophobic surface. The time course of solute exclusion is shown in Fig. 1e.

Microspheres immediately and rapidly translated away from the edges of the Nafion sheet at $\sim 2 \mu\text{m/s}$, leaving an exclusion zone of $600 \mu\text{m}$ within $\sim 10 \text{ min}$. The width of the zone then increased more slowly, commonly expanding to $\sim 1 \text{ mm}$ within 1 day. The images shown in the figure were taken during the early phase of the exclusion process.

The results illustrated in panels c, d and e (Fig. 1) show that the exclusion process does not require a gel; only a surface with hydrophilic moieties is necessary. The apparent hydrophilic requirement implies that the exclusion zone might be initiated through hydrogen bonding with the nucleating surface. This hypothesis was further tested by exposing microsphere suspensions to surfaces that are unable to hydrogen bond with water. No exclusion zones were seen at the interface between silicon rubber and water. Nor were such zones seen adjacent to various metallic wires, including copper, stainless steel, gold, and silver. Fig. 1f shows a representative example.

The range of solutes/particles that could be excluded included not only colloidal microspheres, but smaller species as well. Fig. 2a shows exclusion of fluorophore-labeled serum

albumin, while Fig. 2b shows exclusion of sodium fluorescein dye (Mwt=376). In both cases the ultimate size of the exclusion zone adjacent to the Nafion surface, reached after several

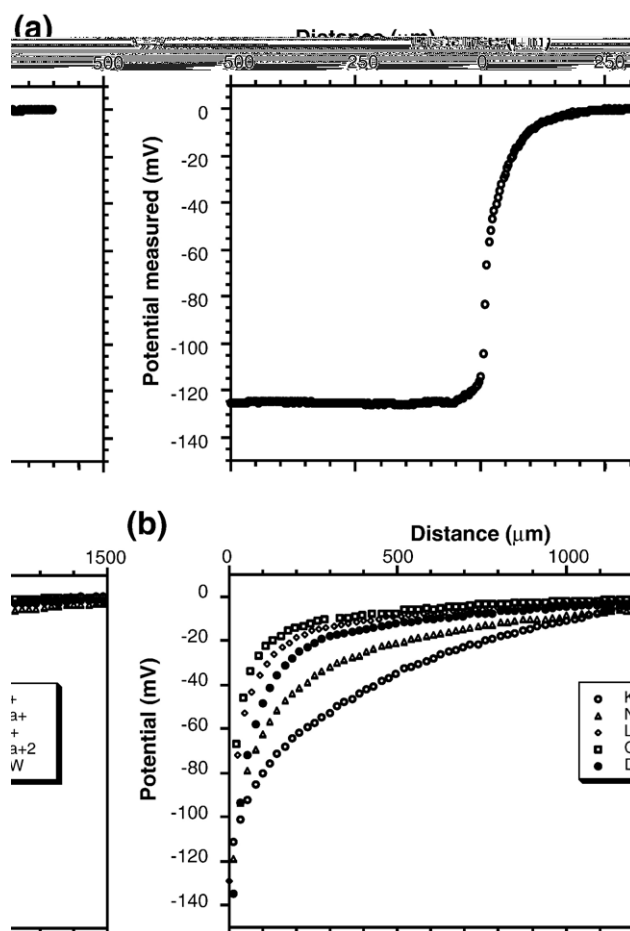


Fig. 3. a. Potential profile as a function of distance from the polyacrylic-acid-gel surface. Surface located at “0” on the abscissa. Inside of gel is to the left of “0”; outside of gel is to the right. Reference electrode is positioned well to the right. b. Potential profile near the Nafion surface, the latter situated at “0” on the abscissa.

minutes, was in the same range as for the microspheres. Thus, exclusion applies not only to colloidal species but also to mid-size and small molecular weight solutes.

2.2. Unique physical characteristics of the exclusion zone

The finding of solute-exclusion zones of size range depicted in Figs. 1 and 2 is to our knowledge unprecedented, although as mentioned, some long-range effects have variously been re-

ported [2,3,9,10]. According to standard DLVO theory, interfacial effects are anticipated to extend no more than nanometers from surfaces [1], but the observations above imply repulsive interactions between surfaces and solutes extending up to six or seven orders of magnitude farther.

While the most obvious source of repulsion is electrostatic, the fact that solute-exclusion zones of 0.3 to 0.4 mm could be found in 150 mM salt solution (Fig. 1b) argues against a purely electrostatic mechanism, for salt ions would be expected to

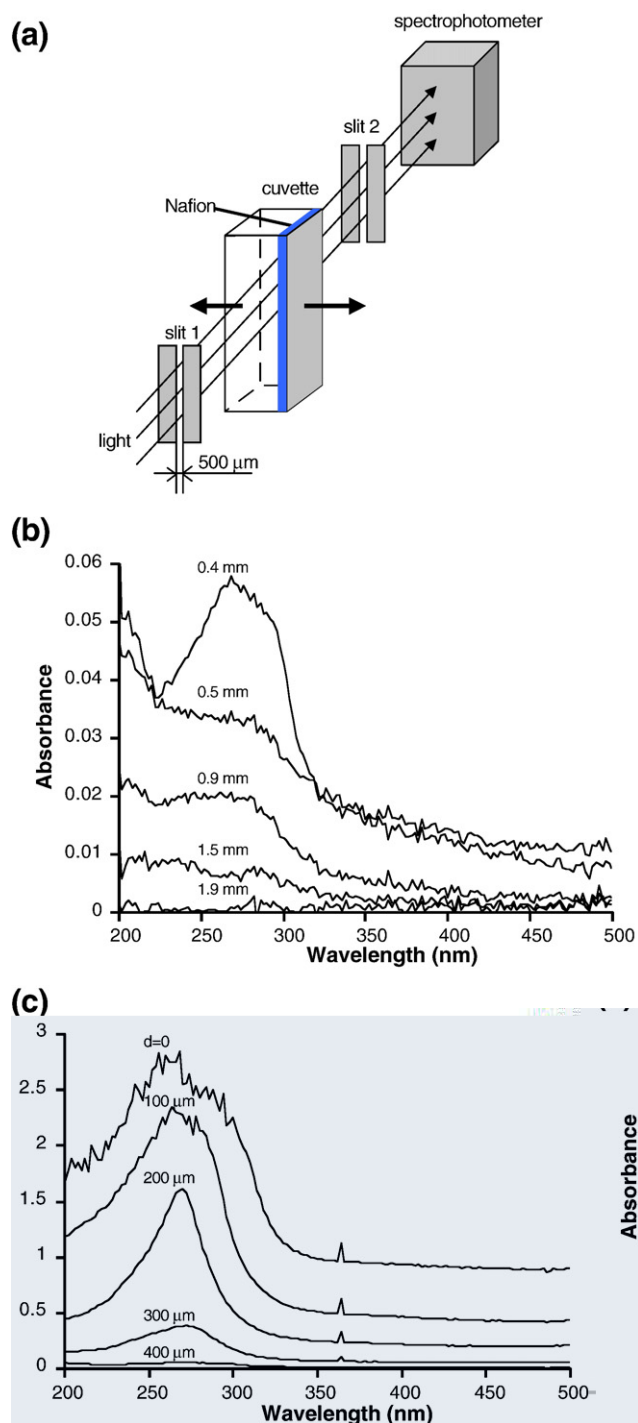


Fig. 4. a. Optical system used to measure UV–Vis spectrum as a function of distance from Nafion surface. b. Spectra measured at varying distances from the Nafion surface. c. Same as b, but closer to Nafion surface. Note difference in scale.

screen surface charges and nullify any such repulsion. Exclusion persists even in solutions containing 0.5 M NaCl (data not shown). Further, we found in some instances that both positively and negatively charged microspheres were similarly excluded from the same surface [20].

An alternative possibility is that the exclusion zone represents a distinct phase of water that excludes solutes. Consistent with this possibility is the observation that solutes of diverse size and character are excluded, ranging from colloidal microspheres to small molecular weight dye. These excluded solutes undergo active thermal motion (visually confirmed in the case of microspheres); yet, they do not diffuse back into the exclusion zone even after days. This maintained separation is not entirely without precedent, for at least in the case of colloidal suspensions of differing composition, phase separation is well recognized [22], as is phase coexistence of mixtures of microsphere solutes of different size [23]. Thus, the gel/polymer/monolayer surfaces could extensively impact the nearby aqueous environment, converting it to a phase that excludes solutes.

To test whether indeed the solute-free phase is physically distinct from the solute-containing phase, we first explored possible differences between exclusion and bulk water through the measurement of potential gradients. Standard 3 M KCl-filled tapered glass microelectrodes were used to measure the potential profile in the vicinity of Nafion and polyacrylic-acid-gel surfaces. A reference electrode was positioned remotely, while the microelectrode tip was advanced with a motor toward the gel surface. With the probe tip positioned well beyond the exclusion-zone boundary, the potential difference was zero. As the probe advanced close enough to the surface, negative potentials began to be registered, their magnitude increasing with increasing proximity of the surface (Fig. 3a and b). In the case of the polyacrylic acid gel (Fig. 3a), the magnitude just outside the gel was ~ 120 mV, and remained steady at that value as the probe advanced inside the gel. In the case Nafion (Fig. 3b), the magnitude rose to (negative) 160 mV at the gel surface, and the profile was altered by the addition of various chloride salts (1 mM). In both situations, non-zero potentials could be detected rather far from the surface: within ~ 200 μm in the case of the gel, and often beyond 1 mm in the case of Nafion.

Thus, sustained potential gradients exist within the exclusion zone, while no such gradients are observable outside that zone. Sustained potential gradients are possible only if mobile charges are not available to screen the charges responsible for creating the potential difference. This appears to be the case within the exclusion zone. Hence, exclusion-zone molecules appear to be stable structures, largely free of mobile charge carriers.

A second way the physical character of the exclusion zone was explored is through measurements of the UV–Vis absorption spectrum. A sheet of Nafion was bonded to one of the four vertical faces of a standard cuvette, which was then filled with distilled, deionized water. The cuvette was positioned such that the Nafion surface was parallel to the optical axis. Incident light passed through vertically oriented slits placed before and after the cuvette, so that we could interrogate narrow windows of the aqueous phase at various distances from the Nafion surface (Fig. 4a). Fig. 4b shows that far from the surface, the spectrum

was flat; i.e., there was no discernible difference between the measured spectrum and that of a blank water sample. However, as the illuminated window came closer to the Nafion, a peak began to appear at ~ 270 nm. The peak grew with proximity to Nafion and eventually dominated the spectrum (Fig. 4c). Hence, absorption features of the interfacial zone differ substantially from those of the bulk zone.

A third way the physical character of the exclusion zone was explored is through examination of infrared emission using a high-sensitivity, high-resolution infrared camera. A Nafion sample was placed in a shallow, water-containing chamber, and allowed to equilibrate for 1 h at room temperature. Infrared radiation from the sample was averaged over multiple image frames and high-pass filtered to remove gradations of overall image brightness.

The results are shown in Fig. 5. They show that the aqueous region immediately adjacent to the Nafion radiates very little (dark), while more distant regions radiate normally (bright). The dark zone extends nominally by 0.3–0.5 mm from the sample surface, which is comparable to the size of the exclusion zone. Infrared radiation intensity is a function of temperature and structure. The former is unlikely to play a significant role, as sustained temperature gradients over small spatial regions are difficult to envision, particularly when records are averaged over extended times. Therefore, the (dark) non-radiating region apparently corresponds to a more stable structure, whose lower emissivity would therefore produce less radiation than ordinary bulk water.

For the fourth method we used magnetic resonance imaging (MRI). A resulting map of apparent transverse relaxation time (T_2) from a multi-echo imaging sequence is shown in Fig. 6; this image is not a T_2 weighted image, but rather, in order to reduce noise, a T_2 fit to a series of images acquired at different echo times.

The apparent T_2 value in the gel is 30.2 ± 0.3 ms; that in the bulk water phase is 27.2 ± 0.4 ms; and that in the interfacial region is 25.4 ± 1 ms. The thickness of the interfacial region is approximately 60 μm , a figure is comparable to the size of the exclusion zone observed with the particular gel (PVA) used. The

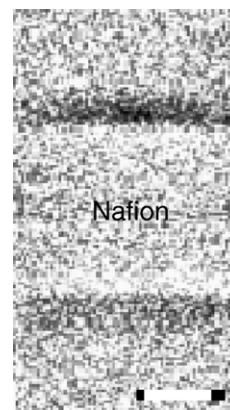


Fig. 5. Infrared radiation image of Nafion-117 in water. Nafion strip runs horizontally (central zone cropped for clarity). Scale: 1 mm between black dots. Darker areas indicate reduced radiation intensity. Interfacial regions, just beyond the edges of the Nafion strip, radiate appreciably less than more remote regions.

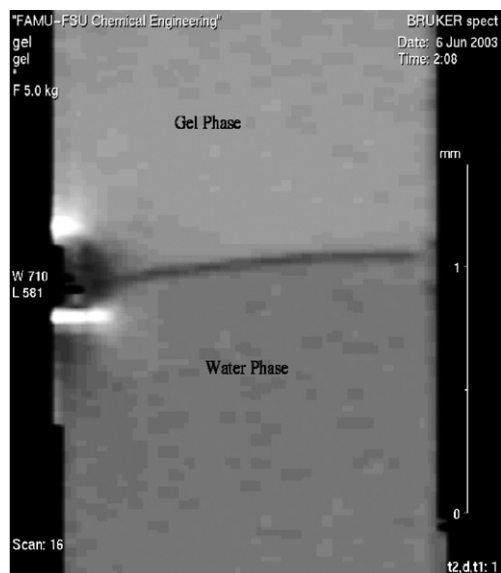


Fig. 6. NMR image of PVA gel (top) and water (bottom) within a cylindrical glass capillary oriented vertically. Air bubble at left. Dark region at interface, $\sim 60 \mu\text{m}$ thick, indicates shorter T_2 value.

fine spatial resolution and small slice thickness for this multi-echo acquisition, make interpretation complex because of the influence of diffusional attenuation; indeed, diffusional attenuation dominates. For lower resolution images obtained on such specimens, the apparent T_2 in the gel phase was substantially shorter than that in the bulk water phase. Pulsed field gradient spin-echo diffusion measurements of water diffusion parallel to the gel–water interface with the same $20 \mu\text{m}$ spatial resolution indicate slightly slower diffusion in the gel phase than in the bulk water phase, and also show the presence of an interfacial region of the same thickness as seen in Fig. 6 in which water diffusion is substantially different from either the bulk water or gel phases. Apparently, water molecules at the interface suffer appreciable restriction.

Evidence presented in Figs. 3–6 reveals that water in the interfacial region has characteristics different from those of bulk water, and that this region extends to unprecedented distances. Further, both IR imaging and MRI results strongly suggest that water molecules in the interfacial zone are considerably less mobile than water molecules in the bulk phase. With the molecular dimension of water at $0.25\text{--}0.3 \text{ nm}$, a nominal $100 \mu\text{m}$ -wide interfacial zone would include a stack of some 3×10^5 water molecules.

2.3. Experimental procedures

2.3.1. Exclusion-zone observations

The reagent solution for synthesizing PAA gels was prepared by mixing 30 ml of 99% acrylic acid (Sigma-Aldrich), 10 ml deionized water, 20 mg N,N' -methylenebisacrylamide (Sigma-Aldrich) as a cross-linking agent, and 90 mg potassium persulfate (Sigma-Aldrich) as an initiator. It was vigorously stirred at room temperature until all solutes were completely dissolved, and then introduced into capillary tubes and sealed; these tubes were

previously washed with ethanol and deionized water. Gelation took place in a water bath as the temperature was slowly raised to about 80°C , and then maintained at the temperature for 1 h to ensure complete gelation. Synthesized gels were carefully pulled out of the capillary tubes. They were then rinsed with deionized water, and stored in a large volume of deionized water, refreshed daily, for 1 week. The PAA gel was placed on a coverslip, superfused with a suspension of $1 \mu\text{m}$ carboxylate-functionalized microspheres, and observed in an inverted microscope (Zeiss Axiovert I35) equipped with a $20\times$ objective.

Skinny rabbit psoas muscle samples were placed in a standard relaxing buffer, ionic strength 150 mM. Microspheres (carboxylate coated, $1 \mu\text{m}$ in diameter, obtained from Polysciences Inc., Warrington, PA) were added to the buffer at a concentration of 0.1%.

Optical fiber FS-SC-7324 (Thorlabs, Newton, NJ) was cleaned repeatedly with lens paper. Then the cleaned optical fiber was inserted into a microsphere suspension of $2 \mu\text{m}$ carboxylate microspheres.

For the monolayer experiments, glass capillary tube, O.D. 1 mm, was coated with gold. Then, an 11-mercapto-undecanoic acid monolayer with COOH-terminus was applied over a 180° zone running the full length of the tube, leaving a half-cylinder covered with monolayer, the other half only with gold. The capillary tube was placed boundary down, on a glass slide containing a large droplet of a $1\text{-}\mu\text{m}$ amidine-functionalized microsphere suspension, and covered with a glass cover slip.

For the Nafion experiment, Nafion-117 film, spear shaped, $170 \mu\text{m}$ thick (Aldrich, Milwaukee, WI), was sandwiched between two glass cover slips, much larger than the film specimen. A carboxylate-functionalized microsphere suspension was infiltrated around the sandwiched film.

For the *metal-surface observations*, a stainless steel wire was placed between two cover slips. A carboxylate-functionalized microsphere suspension $2\text{-}\mu\text{m}$ diameter was infiltrated around the sandwiched film.

2.3.2. Exclusion of protein and fluorescein

Fluorescent albumin (Sigma-Aldrich) or Na fluorescein (Sigma-Aldrich) was added to solution exposed to a Nafion surface. Development of the exclusion zone was monitored with fluorescence microscopy.

2.3.3. Potential measurement

Standard 3 M KCl-filled tapered glass microelectrodes were used to measure the potential profile in the vicinity of Nafion and polyacrylic-acid-gel surfaces. A reference electrode was positioned remotely, while the microelectrode tip was advanced with a motor toward the gel surface at a speed of $30 \mu\text{m/s}$.

2.3.4. Spectrophotometer

The incident light of an HP 8452A diode-array spectrophotometer was shaped by two vertical slits $100 \mu\text{m}$ width, separated by 30 cm. Between the slits was placed the UV cell. Cell position was adjustable with a precision of $10 \mu\text{m}$. The Nafion surface was adjusted parallel to the light beam. The reference spectrum was taken at a position far from the Nafion

surface inside the cell filled with deionized water. By changing the position of the cell, a series of spectra was obtained.

2.3.5. MRI

Polyvinyl alcohol (PVA) gels were prepared by alternate freezing and thawing of a 3/7 mixture of 10% by wt. PVA solution in water and 10% by wt. PVA solution in dimethyl sulfoxide (DMSO). The mixed solution was injected into a mold to retain the shape either in the form of a rod 0.5 mm in diameter (for configuration *A*), or as a rectangular cube with a 1-mm cylindrical hole (for configuration *B*). Solutions were stored in a freezer (−20 °C) for 23 h for physical cross-linking, and then exposed to air at room temperature for 1 h of annealing. This cycle was repeated four times. Finally the gels were purified by five alternating cycles of immersion in acetone and deionized water, and then stored in a large bath of pure water for at least 2 days. The obtained gels were transparent and had almost the same index of refraction as water. Cylindrical polyvinyl alcohol gels were inserted into glass tubes whose inner diameters slightly exceeded those of the gel, leaving a length of tube that could be filled with water. The tube was sealed at both ends, and imaged on a Bruker 500 MHz DRX microimaging NMR spectrometer at room temperature. Spatial resolution in the acquired images was 20 μm.

2.3.6. Infrared radiation imaging

Infrared-camera spectral window: 3.8–4.6 μm. Spatial resolution 320×240 pixels/frame. Temperature noise equivalent (limited by camera noise) 0.015 K at 200 frames/s sampling rate. Averaging of 100–200 frames reduced noise equivalent to 0.001 K, which is an order of magnitude smaller than the measured temperature-equivalent difference.

All experiments were carried out at room temperature.

3. Conclusions

The finding of large zones of mobility-limited water carries broad implication for biology, biotechnology, and other realms. In the cell, for example, extreme crowding implies that the aqueous phase may be entirely interfacial [7,24,25], and if the interfacial phase excludes solutes, then some mechanism would be required to permit solute–surface interactions, including those between substrates and enzymes. Indeed, the possibility of water impacted by surfaces raises the question of long-range recognition of complementary entities such as enzymes–substrates, antigens–antibodies, etc. In the area of friction and nano-tribology, parallel surfaces shearing past one another undergo stick–slip behavior, which is known to arise from the intervening fluid's restriction–relaxation cycles [26–29]. The present results anticipate the restriction phase, and give direction toward understanding the genesis of low friction. In the area of colloid chemistry, understanding why even relatively dilute suspensions of colloidal solutes converge into quasi-regular arrays [15–17] could reside in the extensiveness of mobility-limited water surrounding these particles. If so, then water organization around charged surfaces could be a key attribute underlying biological and bio-inspired self-organization. In various common bioseparation technologies

such as chromatography, the presence of solute-exclusion zones around gel beads raises questions about the conventionally accepted separation mechanism; understanding the role of solute exclusion could lead to important technological advances. Finally, anti-fouling agents against various biofilm formations and their applications to common biomaterials may well originate in the exclusion phenomenon observed here.

In sum, hydrophilic interfaces play a role more profound than generally assumed. Solutes in aqueous suspension are extensively excluded from the vicinity of many interfaces, and the evidence presented here supports the view that such exclusion arises from long-range restriction of water molecules, nucleating at the interface and projecting well into the aqueous phase, similar to what occurs in liquid crystals. The presence of such unexpectedly large zones of mobility-limited water must impact many features of surface and interfacial chemistry.

Acknowledgments

We thank Steven Gibbs, National High Magnetic Field Laboratory, Florida State University, Tallahassee, FL, for his assistance with the magnetic resonance experiments. We also acknowledge constructive comments along the way from Philip Ball, Mark Banaszak Holl, Frank Borg, David Burns, Charles Campbell, Angela Carden, Ben Chu, Jim Clegg, Ferenc Horkay, Jacob Israelachvili, Noah Lotan, Mickey Schurr, Jan Spitzer, Andy Symonds, Erwin Vogler, John Watterson, Philippa Wiggins, and Jennifer Whittier. This study was supported by grants from NIH (5R21AT002362-02 and 5R21AT002635-01A1) and ONR (N00014-05-1-0773) to GHP and WCC. WCC was also supported by an ABMR award.

References

- [1] Israelachvili J. *Intermolecular and Surface Forces*. San Diego: Acad. Press; 1992.
- [2] Asakura S, Oosawa F. *J Polym Sci* 1958;33:183.
- [3] Crocker JC, Matteo JA, Dinsmore AD, Yodh AG. *Phys Rev Lett* 1999;82:4352.
- [4] Henniker JC. *Rev Mod Phys* 1994;21:322.
- [5] Szent-Gyorgyi A. *Bioenergetics*. New York: Acad. Press; 1957.
- [6] Ling GN. *In Search of the Physical Basis of Life*. New York: Plenum; 1984.
- [7] Pollack GH. *Cells, Gels and the Engines of Life: A New, Unifying Approach to Cell Function*. Seattle: Ebner and Sons; 2001.
- [8] Clegg JS, Drost-Hansen W. In: Hochchka PW, Mommsen TP, editors. *Biochemistry and molecular biology of Fishes*. Amsterdam: Elsevier; 1991.
- [9] Ito K, Yoshida H, Ise N. *Science* 1994;263:66.
- [10] Yoshida H, Ise N, Hashimoto T. *J Chem Phys* 1995;103:10146.
- [11] Pashley RM, Kitchener JA. *J Colloid Interface Sci* 1979;71:49.
- [12] Fisher IR, Gamble RA, Middlehurst J. *Nature* 1981;290:575.
- [13] Ling GN. *Physiol Chem Phys Med NMR* 2003;35:91.
- [14] Roy R, Tiller WA, Bell I, Hoover MR. *Mater Res Innov* 2005;9:1066.
- [15] Ito K, Nakamura H, Yoshida H, Ise N. *J Am Chem Soc* 1988;110:6955.
- [16] Ise N, Konishi T, Tata BVR. *Langmuir* 1999;15:4176.
- [17] Ise N, Matsuoka H, Ito K, Yoshida H. *Faraday Discuss Chem Soc* 1990;90:153.
- [18] Negendank W. *Biochim Biophys Acta* 1982;694:123.
- [19] Wiggins PM. *Microbiol Rev* 1990;54:432.
- [20] Zheng J-M, Pollack GH. *Phys Rev E* 2003;68:1.

- [21] Heitner-Wirguin J. *Membr Sci* 1996;120:1.
- [22] Albertsson PA. *Partition of Cell Particles and Macromolecules*. NY: Wiley; 1960.
- [23] Kaplan PD, Rouke JL, Yodh AG, Pine DJ. *Phys Rev Lett* 1994;72:582.
- [24] Clegg JS. *Am J Physiol* 1984;246:R133.
- [25] Clegg JS. In: Jones DP, editor. *Microcompartmentation*. Boca Raton: CRC Press; 1998.
- [26] Yoshizawa H, Israelachvili J. *J Phys Chem* 1993;97:11300.
- [27] Gee M, McGuiggan P, Israelachvili JN. *J Chem Phys* 1990;93:1895.
- [28] Thompson P, Robbins M. *Science* 1990;250:792.
- [29] Diestler D, Schoen M, Cushman J. *Science* 1993;262:545.